Energy & Buildings 280 (2023) 112737

Contents lists available at ScienceDirect

Energy & Buildings

journal homepage: www.elsevier.com/locate/enb

Energy and exergy analysis of an experimental ventilated façade

Ana Picallo-Perez *, José María Sala-Lizarraga

University of the Basque Country, ENEDI Research Group, Energy Engineering Department, Pl. Ingeniero Torres Quevedo 1, 48013 Bilbao, Spain

ARTICLE INFO

Article history:
Received 19 October 2022
Revised 8 December 2022
Accepted 19 December 2022
Available online 21 December 2022

Keywords:
Ventilated façade
Experimental test
Exergy analysis
Performance indexes

ABSTRACT

This work, analyzes ventilated façades through the first and second law of thermodynamics. In addition to the energy-balances, it presents the exergy-balances on the interior and exterior surface of a façade, taking into account the different mechanisms of heat exchange. It proposes two new indexes (EQC and ExQC) to characterize the behavior of ventilated façades, by comparing their behavior with a reference façade and considering the energy balance in one case and the exergy balance in the other. An experimental test of a forced ventilated façade serves as the case study, using the test-methodology based on Paslink cells. The test data serve to characterize the behavior of the façade, both from an energy and exergy point of view. Overall, 53.05 kWh of heat is lost to the outside through the façade during 6 days of November, which corresponds to 0.31 kWh of exergy-loss. The internal energy change of the façade is decomposed according to its layers, showing that in terms of energy the sandwich insulation layer influences the most (99.45 % of the total change) but in terms of exergy, on the contrary, the metal sheet affects the most (83.66 %). The values obtained for the two indexes show that, under the test conditions, although the ventilated façade and the reference façade present similar values from the energy point of view, when the exergy is used, it is clearly seen that the behavior of the ventilated façade is 44 % better.

1. Introduction

The population does not value comfort homogeneously when responding about thermal and air quality aspects. Therefore, balance parameters and strategies are established to supply a common comfort level-range within architectural design. As a rule, comfort is guaranteed when the body temperature is within a certain range, the skin has a low humidity and the physiological effort of regulation is minimum. The active and passive systems of buildings are responsible for maintaining thermal comfort by consuming natural resources, so their role is essential to sustaining society itself. Consuming natural resources involves using renewable or fossil fuels, although these last emit greenhouse gases and contribute to climate change. Currently, buildings account for about 40 % of the total energy consumption and 36 % of the CO_2 emissions in the European Union [1]. To reduce these consumptions, passive solutions can be used by involving the building's architecture.

Ventilated Façades (VF) [2] are constructive solutions, which can be incorporated in refurbishment or new buildings, and improve the energy efficiency of the buildings to help ensure indoor comfort. They are based on a double skin with an air chamber which slows down the rate of heat transfer. On the one hand, heat is stored in a thermal mass-wall and is conducted, radiated and transmitted to the interior space that is being acclimatized. On the other hand, VF extracts the thermal energy of the heated air directly to the outside, or introduces it into the interior through the openings at the ends of the façade. This air moves between the dampers by natural convection or can be forced and controlled by fans. More and more prefabricated slabs and façade modules are becoming available due to advances in production, which offer the opportunity to implement VF modules more easily, as is the case of Ref. [3], which studies the renovation of a high school building with prefabricated VF elements.

The work in Ref. [4] studies and discusses the most recent and cutting-edge research into double-skin façades for building retrofit. VFs provide a thermal buffer zone, energy savings and other benefits. Ref. [5] theoretically compares the energy performance of an Opaque Ventilated Façade against a conventional one through a CFD analysis, considering two specific days, different orientations and two wind-velocities; the work concludes that the VF saves between 20 and 55 % of energy compared to the conventional one. Ref. [6] also uses CFD simulations and optimizes a novel opaque dynamic façade, with an integrated ventilation module, phase change materials and an adjustable insulation system. As an outcome, the airflow can increase or decrease the thermal resistance of the façade to control the heat loss along the year. Maciel and

* Corresponding author.
E-mail address: ana.picallo@ehu.eus (A. Picallo-Perez).

https://doi.org/10.1016/j.enbuild.2022.112737
0378-7788/

Carvalho [7] develop a methodology to compare opaque ventilated façades to cladding façades based on several simulations and statistical processing data. Ref. [8] also studies opaque ventilated façades, through a sensitivity analysis, to evaluate the performance and influence of the outdoor boundary conditions. The state-of-the-art overviewed in the work highlights that, after 2011, the experimental energy-analysis of naturally ventilated façades is the most widespread approach in the literature. Ref. [9] studies different wall layer properties and their effect on the thermal performance of ventilated façades by measuring heat flow and ventilation. As a result, the presence of an internal mass increases the heat transfer towards the indoor environment. The study of Ref. [10] evaluates the design, construction and thermal performance of an experimental VF. As it aims to keep the principles of the circular economy, all the materials are bio-based. As a result, this façade is a promising option for warm climates. An opaque ventilated façade made up of recycled materials is tested during a winter period in Ref. [11]. This work does a hygro-thermal analysis to account for heat losses as well as to control the moisture.

As mentioned above, throughout the published literature review, a large number of works analyze experimentally the behavior of VFs; the most recent works design VFs with innovative materials and special characteristics, and many of the works perform the analysis dynamically. However, all the literature focuses on energy studies, based on the first law of thermodynamics, but no work has been found that applies the second law introducing the exergy property in ventilated façades solutions.

Indeed, the exergy method is a well-established thermodynamic method that helps to improve the efficiency of processes. However, its application in buildings is not as popular as energy analyses. This exergy analysis can be applied either at facility level, building level or even for urban planning. One of the most detailed publications applying exergy in buildings appears in Ref. [12], which details the application of exergy, both in the building envelope and in its facilities. As with energy analysis, exergy analysis aims to search for techniques that reduce fossil fuel consumption, increase the use of renewable energy and use energy more efficiently. In addition, it provides additional information to conventional energy analysis, thus uncovering energy and environmental problems and therefore bringing about better design solutions.

Although VF exergy analyses rarely appear in the literature, there are a few papers that refer to the second law of thermodynamics applied to buildings envelope. Ref. [13] simulates a triangular-roof enclosure to obtain the numerical solution of the entropy production due to natural convection. Ref. [14] also deals with mathematical approaches and remarks the importance of second law analyses to evaluate the quality of energy sources in order to get better strategies for building designs. Therefore, the work analyzes thermal exergy flows through the building and defines the human body exergy balance. Human body exergy balances are also deeply developed in Ref. [15]. Low-exergy buildings are defined and simulated in Ref. [16] and the detailed analysis of a building envelope appears in Ref. [17]; this work simulates four different building envelops and compares the exergy analysis results. Ref. [18] analyzes the envelope and the heating system of a nZEB in Spain under the exergy point of view; the results show the possibilities for energy efficiency improvement that cannot be appreciated with pure energy analysis. The entire heating process in buildings is investigated in Ref. [19], from the exergy of the building envelope, room air, heat energy emission system, distribution, storage, generation system, until the primary energy transformation, dealing with the simulation results. Something similar is done in Ref. [20], which compares the energy and exergy performances of an old and a retrofitted building in Spain, from the envelope until the primary energy, or in Ref. [21] which studies a low exergy heating system from the ground-source heat pump to the building envelope. Ref. [22] defines the mathematical model for applying dynamic exergy and exergoeconomic analyses to the building envelope, to calculate the heating and cooling demands. Unsteady-state exergy analysis, based on a finite difference software, are also applied in Ref. [23] on externally and internally insulated envelopes to have new insights for the buildings design.

The review of heat transfer and energy flow characteristics of the building envelopes in Ref. [24] concludes that exergy analysis becomes more significant and helpful with active envelops, i.e., in buildings with integrated PV (BIPV) or thermal (BIPV-T) solutions. In a similar way, Ref. [25] reviews the present day application of BIPV and BIPV-T technologies under the energy and exergy perspectives. The performance of semi-transparent hybrid photovoltaic thermal double pass façades (HPVT-DPF) are energetically and exergetically analyzed in Ref. [26] by results obtained from simulations. In addition, Ref. [27] evaluates the building integrated semitransparent photovoltaic (BISPV) modules for roof and façade, to determine the energy and exergy performance of the building. A building with BIPV-T is also simulated in Ref. [28] where the dynamic exergy analyses of all the system components is done and is compared to a reference building model, i.e., a building without BIPV-T. The work points out that usually exergy studies are focused only on the BIPV-T collector itself, disregarding the whole building-plant.

2. Objective and methodology

As justified in the previous introduction section, some works (1) analyze the VFs from an energy point of view and (2) several studies relate the envelope thermal losses to the exergy analysis; however, we have not found works linking these two fields together. The following points summarize the reviewed literature in order to get a generic picture of the state of the art:

- Referring to (1) VFs analysis:
  - As described in Refs.[4–11], the recent works experimentally characterize ventilated façades only from the energy point of view; all these papers are published during the last two years, 2020–2022.
- Referring to (2) exergy analyses in buildings envelope:
  - These works are scarcer so the literature review has been extended from 2009 to 2020, and no work has been found after that 2020 year.
  - As marked in Refs.[22,23], the majority of studies in the literature follow a steady-state approach when conducting an exergy analysis by fixing a constant reference temperature. Nevertheless, there is a necessity of making a dynamic analysis because of the environmental conditions change.
  - Most of the works [13,17,19,21–23,26,28] are associated with simulation results, since it is often not possible to validate the energy and exergy performance with experimental data.
  - The works of Refs.[13–16,18–21,24–28] develop the mathematical formulae to define the exergy losses through façades, focusing exclusively on the losses from the interior to the exterior, without considering the type of façade under analysis nor the composition of its specific layers.

Therefore, this work aims to fill the research gap of VFs analysis with the following objectives and novelties:

- To define the mathematical formulae for applying dynamic energy and exergy analyses in VFs.
- To propose new indexes, EQC and ExQC, to characterize the energy and exergy behaviour of a VF versus a conventional one.

- To carry out an experimental dynamic essay of a forced VF in a Paslink test-cell, to obtain the corresponding dynamic data at each layer of the façade.
- To apply the proposed balances and indexes to the forced VF tested.

Therefore, this work explains how to apply the exergy methodology to characterize the thermal behavior of a VF, after doing the corresponding energy analysis.

The structure of the work appears in Fig. 1. After the introduction of Section 1 and the work justification in Section 2, Section 3 develops the energy and exergy balances in the internal and external surfaces of a conventional façade, taking into account all the different heat transfer mechanisms. Based on these expressions, the work formulates the energy and exergy balances for a VF in Section 4 and defines some indexes that characterize its behavior versus a conventional façade. Section 5 describes the characteristics of the test performed on a VF in a PASLINK test-cell, together with their corresponding data obtained. Section 6 presents the numerical results of the energy and exergy behavior and shows the values of the performance coefficients and finally, Section 7 highlights the conclusions of the work and Section 8 contains the discussion.

3. Energy and exergy balances in the surfaces of a conventional façade

The following section contains the mathematical approach to characterize a façade through its energy and exergy balances. According to the adopted sign convention, the heat flux that reaches the surface is considered positive and the flux that comes out is negative.

3.1. Energy balance in the internal surface

If an energy balance is applied to the internal surface of the façade in winter conditions, when the outdoor temperature T_0 is lower than the indoor temperature T_i ($T_0 < T_i$), heat goes from the inside through the façade, see Fig. 2 (a):

$$\dot{Q}_{r,lw,is} + \dot{Q}_{r,sw,is} + \dot{Q}_{cv,is} = \dot{Q}_{cd,is} \tag{1}$$

where:

- $\dot{Q}_{r,lw,is}$: corresponds to the exchanged longwave radiation (by absorption - emission). This term includes the exchanges with the other interior surfaces at different temperatures, as well as the radiant exchange with the internal heat sources, without considering lighting.
- $\dot{Q}_{r,sw,is}$: represents the redistributed and absorbed shortwave radiation; it considers contributions from the sun (through the openings) and from internal sources, such as lighting.
- $\dot{Q}_{cv,is}$: represents the heat exchanged by convection with the indoor air.
- $\dot{Q}_{cd,is}$: refers to the heat transfer by conduction through the façade.

The analysis of the radiant exchange of interior surfaces is complex due to the different surfaces and natures of this radiation. Therefore, the $\dot{Q}_{cv,is}$ convection and $(\dot{Q}_{r,lw,is} + \dot{Q}_{r,sw,is})$ radiation fluxes are considered to be parallel, so a combined convection-radiation coefficient $h_{cv-r,is}$ is used to simplify the calculation and to consider the heat flux directly through Newton's cooling equation.

$$h_{cv-r,is} = h_{cv} + h_r \tag{2}$$

$$\dot{Q}_{is} = A h_{cv-r,is}(T_i - T_{si}) \tag{3}$$

where A is the heat transfer area and h_r is an equivalent radiation coefficient, being $h_r = 4\sigma\varepsilon_{is}\bar{T}_m^3$; $\bar{T}_m = (T_{si} + \bar{T}_{sj})/2$ and $\bar{T}_{sj}$ is the average of the other internal surface temperatures that exchange radiation with the surface considered, σ is the Boltzmann constant, and ε_{is} is the emissivity of the internal surface considered.

In Spain, the Technical Building Code (CTE) [29] limits the maximum thermal transmittance values $K_{lim}\left[W/m^2K\right]$ that buildings can have through standardized convection-radiation coefficients $h_{cv-r,is}$, whose values take into account whether the flow is horizontal or vertical (ascending or descending), see Table 1.

In order to calculate K_{lim}, the characteristics of each element that make up the thermal envelope need to be included, taking into account the compactness and its heat exchange surface with the exterior. Therefore, the calculation is on the basis of each element, which in turn must comply with a limiting thermal transmittance ($U_{lim}\left[W/m^2K\right]$) [30].

Knowing the $h_{cv-r,is}$ coefficient and the internal surface temperature T_{is}, the energy balance results as:

$$A h_{cv-r,is}(T_i - T_{is}) = \dot{Q}_{cd,is} \tag{4}$$

3.2. Exergy balance in the internal surface

Referring now to the exergy balance in the interior surface:

$$\dot{B}_{r,lw,is} + \dot{B}_{r,sw,is} + \dot{Q}_{cv,is}\left(1 - \frac{T_0}{T_i}\right) = \dot{Q}_{cd,is}\left(1 - \frac{T_0}{T_{is}}\right) + \dot{D}_{is} \tag{5}$$

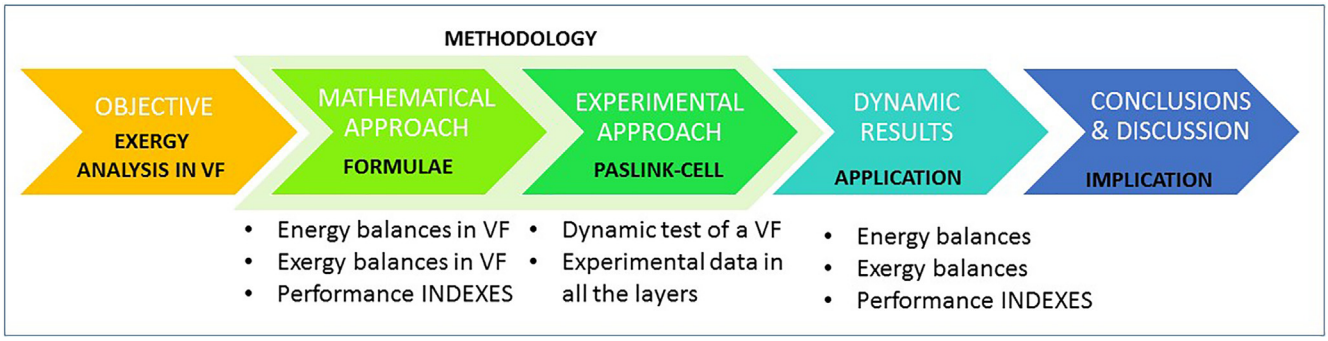

Fig. 1. Summary of the work structure.

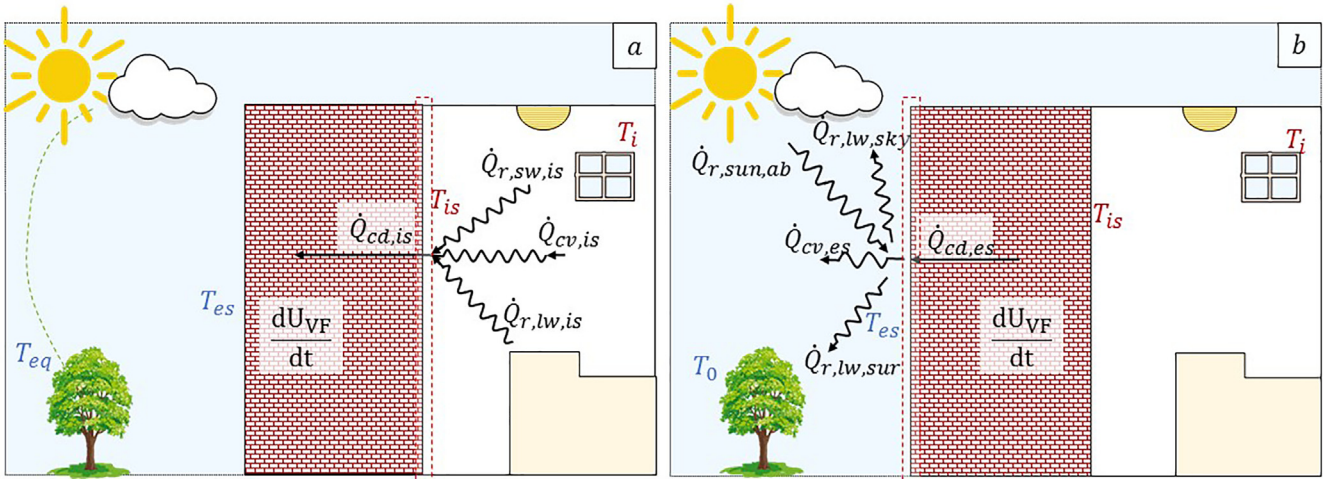

Fig. 2. (a) Energy balance in the internal surface and (b) in the external surface of the façade.

Table 1
Maximum thermal transmittance values according to CTE.

K_{lim} [W/m²K]	Compactness	Winter climate zone					
	V/A [m³/m²]	α	A	B	C	D	E
New buildings and expansions	V/A ≤ 1	0.67	0.6	0.58	0.53	0.48	0.43
	V/A ≥ 4	0.86	0.8	0.77	0.72	0.67	0.62
Changes in use	V/A ≤ 1	1	0.87	0.83	0.73	0.63	0.54
Renovations of more than 25 % of the total envelope area.	V/A ≥ 4	1.07	0.94	0.9	0.81	0.7	0.62

where $\dot{B}_{r,lw,is}$ and $\dot{B}_{r,sw,is}$ designate the exergy of longwave and shortwave radiation exchanged by the internal surface respectively, T_0 is the dead state temperature, and $\dot{D}_{is}$ is the rate of exergy destruction at the internal surface. This destruction is due to (1) absorption of longwave radiation from the rest of the interior surfaces, (2) emission from the surface itself, (3) redistributed shortwave absorption from the sun, (4) from lights and (5) exergy destruction associated with convection in the boundary layer between the air and the surface.

Annex 49 [31] recommends using the properties of the "air around the building" to define the dead state temperature, because when the indoor air (in imbalance with the outdoor air) passes through the façade, it destroys all its exergy until it reaches equilibrium with the outdoor environment. Therefore, as said, the surrounding ambient-air can be considered as the source or sink for the energy processes of buildings and their facilities, always keeping in mind the dynamic behavior of the building and of the outdoor temperature.

Although the radiation and convection exchanged have different thermodynamic qualities, in a first approximation, the convection-radiation coefficient $h_{cv-r,is}$ is considered for a combined $\dot{Q}_{is}$ term. Then, as the exergy flux that arrives on one side of the surface is greater than the exergy flux that leaves on the other side, the difference is the rate of exergy destruction that takes place on the surface:

$$A\,h_{cv-r,is}(T_i - T_{is})\left(1 - \frac{T_0}{T_{is}}\right) = \dot{Q}_{is}\left(1 - \frac{T_0}{T_{is}}\right) = \dot{Q}_{cd,is}\left(1 - \frac{T_0}{T_{is}}\right) + \dot{D}_{is} \quad (6)$$

In summer, when $T_0 > T_i$, the same exergy balance equation applies, but now the exergy associated with the energy exchanged has the opposite sense and this can be seen algebraically in eq. (6), as the coefficient $\left(1 - \frac{T_0}{T_{is}}\right)$ has a negative sign.

3.3. Energy balance in the external surface

If the formulae focus on the external surface of the façade, under winter conditions, there will be a net heat flow by conduction from inside the façade to the external surface, see Fig. 2 (b), and as the heat flux is the same on one side of the surface as on the other:

$$\dot{Q}_{cd,es} = \dot{Q}_{r,lw,sky} + \dot{Q}_{r,lw,sur} + \dot{Q}_{cv,es} - \dot{Q}_{r,sun,ab} \quad (7)$$

where:

- $\dot{Q}_{cd,es}$ corresponds to the rate of heat by conduction from the interior of the wall to the external surface.
- $\dot{Q}_{cv,es}$ is the rate of heat exchanged by convection with the outside air.
- $\dot{Q}_{r,sun,ab}$ is the rate of shortwave radiation absorbed from the sun (inward (-)).
- $\dot{Q}_{r,lw,sky}$ is the rate of longwave radiation exchanged with the sky.
- $\dot{Q}_{r,lw,sur}$ is the rate of longwave radiation exchanged with the surroundings, such as the ground, other buildings, etc.

In the same way as in the interior surface, a $h_{cv-r,es}$ coefficient can be defined to combine $\dot{Q}_{cv,es}$ convection and $(\dot{Q}_{r,lw,sky} + \dot{Q}_{r,sur})$ longwave radiation, and introducing the equivalent temperature T_{eq} [12]:

$$h_{cv-r,es} = h_{cv} + 4\sigma\varepsilon_{es}T_m^3 \quad (8)$$

$$T_{eq} = T_0 + \frac{\varepsilon_{es}\sigma T_0^4\left(F_{es,sky}\varepsilon_{sky} + F_{es,sur} - 1\right)}{h_{cv-r,es}} \quad (9)$$

$$\dot{Q}_{r,lw,sky} + \dot{Q}_{r,lw,sur} + \dot{Q}_{cv,es} = h_{cv-r,es}\left(T_{eq} - T_{es}\right) \quad (10)$$

where:

- ε_{es} is the emissivity of the external surface,
- σ is the Stefan-Boltzmann coefficient,
- T_m is the arithmetic mean of T_{es} and T_0 to linearize the $T_{es}^4 - T_0^4$ expression,
- ε_{sky} is the emissivity of the celestial vault calculated as $\varepsilon_{sky} = \varepsilon_0 + 0.8(1-\varepsilon_0)C_{cloud}$, C_{cloud}being the cloudiness factor and ε_0 the equivalent emissivity corresponding to a clear sky [32].
- $F_{es,sky}$ and $F_{es,sur}$ are the vision factors surface/sky and surface/surroundings respectively.

Then eq. (7) becomes:

$$\dot{Q}_{cd,es} = h_{cv-r,es}(T_{eq} - T_{es}) - \dot{Q}_{r,sun,ab} \tag{11}$$

The shortwave radiation from the sun absorbed by the exterior surface $\dot{Q}_{r,sun,ab}$ is:

$$\dot{Q}_{r,sun,ab} = \alpha_{es} G_T A \tag{12}$$

where α_{es} is the absorptivity for shortwave radiation of the exterior surface, G_T is the solar irradiation $\left[\frac{W}{m^2}\right]$, and A is the surface. It is composed of direct and diffuse radiation (with different associated exergies) and its value depends on location, orientation, day and time.

3.4. Exergy balance in the external surface

In the same way as eq.(7), an exergy balance on the external surface gives:

$$\dot{Q}_{cd,es}\left(1 - \frac{T_0}{T_{es}}\right) = \dot{B}_{r,lw,sky} + \dot{B}_{r,lw,sur} + \dot{Q}_{cv,es}\left(1 - \frac{T_0}{T_{es}}\right) - \dot{B}_{r,sun,ab} + \dot{D}_{es} \tag{13}$$

The exergy fluxes referring to the exchange of longwave radiation between the sky $\dot{B}_{r,lw,sky}$ and the exterior surface-surroundings $\dot{B}_{r,lw,sur}$ can be combined through the fictitious temperature $T_{f,sky}$ as follows:

$$T_{f,sky} = (1 - F_{es,sky})T_{sur} + F_{es,sky}T_{sky} \tag{14}$$

and, using the Petela expression to calculate the exergy of radiation:

$$\dot{B}_{r,lw,sky} + \dot{B}_{r,lw,sur} = A\,\varepsilon_{es}\sigma\left(T_{es}^4 - T_{f,sky}^4\right)\left[1 - \frac{4}{3}T_0\frac{\left(T_{es}^3 - T_{f,sky}^3\right)}{\left(T_{es}^4 - T_{f,sky}^4\right)}\right] \tag{15}$$

Many energy analyses also combine the short and longwave radiation mechanisms with convection into a single term, to apply Newton's cooling law by the convection-radiation coefficient, and the sun-air temperature [12]. However, although using the $h_{cv-r,is}$ coefficient in the exergy balance of the internal surface (eq. (6)), encompassing short- and longwave mechanisms in the external surface is not adequate for the exergy calculation, due to the various thermodynamic qualities of these energy transfers. Nevertheless, longwave radiation exergy flows can be joined with the external convection mechanism through the $h_{cv-r,es}$ convection-radiation coefficient in the $\dot{B}_{es}$ term,

$$\dot{B}_{es} = \dot{B}_{r,lw,sky} + \dot{B}_{r,lw,sur} + \dot{Q}_{cv,es}\left(1 - \frac{T_0}{T_{es}}\right) = Ah_{cv-r,es}(T_{eq} - T_{es})\left(1 - \frac{T_0}{T_{es}}\right) \tag{16}$$

Thus, summarizing the exergy balance stays as follows:

$$\dot{Q}_{cd,es}\left(1 - \frac{T_0}{T_{es}}\right) = \dot{B}_{es} - \dot{B}_{r,sun,ab} + \dot{D}_{es} \tag{17}$$

where, following Petela

$$\dot{B}_{r,sun,ab} = \alpha_{es}AG_T\left\{1 + \frac{1}{3}\left(\frac{T_0}{T_{sun}}\right)^4 - \frac{4}{3}\frac{T_0}{T_{sun}}\right\} \tag{18}$$

andT_{sun} = 5.700 K is the solar radiation temperature approximated to a black body. As mentioned above, for a more accurate analysis, G_T should be decomposed into direct and diffuse irradiance [12].

The net heat-loss through the exterior surface is finally exchanged with the environment by convection and longwave radiation until it reaches the ambient temperature T_0 (the dead state). Thus, the exergy of this heat-loss is completely destroyed in the environment, resulting in an exergy loss:

$$\dot{Q}_{cd,es}\left(1 - \frac{T_0}{T_{es}}\right) + \dot{B}_{r,sun,ab} = \dot{L}_{es} \tag{19}$$

In winter, the conduction heat flux in the external surface and its exergy have the same sense, both are from the interior to the exterior, while in summer the conduction heat flux in the external surface is inward, whereas its associated exergy flow, on the contrary, is outward.

4. Thermodynamic analysis of a ventilated façade

Ventilated façades incorporate insulation together with a ventilated air chamber, with an outer sheet joined to the interior by means of a substructure, see the scheme of Fig. 3.

The air chamber is the primary component of the system, performing various functions: it prevents the dynamic forces of the wind from reaching the interior components, it acts as a drainage system against eventual infiltrations, it allows the evacuation of water vapor coming from the perspiration of the enclosure of the building and, likewise, the circulation of air cools the excess of solar radiation incident on the skin of the cladding.

4.1. Energy and exergy balances in a ventilated façade

According to the above nomenclature, from an energy balance in a non-stationary state, considering the whole façade as a control volume and that heat goes from the exterior to the interior, the following equation is written:

$$\frac{dU_{VF}}{dt} = \dot{Q}_{r,sun,ab} + \dot{Q}_{cv-r,es} - \dot{Q}_{cv-r,is} + \dot{H}_{in} - \dot{H}_{out} \tag{20}$$

$$\frac{dU_{VF}}{dt} = A\alpha_{es}G_T + Ah_{cv-r,es}(T_{eq} - T_{es}) - A\,h_{cv-r,is}(T_{is} - T_i) + \dot{H}_{in} - \dot{H}_{out} \tag{21}$$

where U_{VF} is the internal energy accumulated in the materials that make up the façade, which can be calculated knowing the temperature T_j, the thermal capacity c_{P_j} and the mass m_j of each j- layer; and $\dot{H}_{in}$ and $\dot{H}_{out}$ are the rate of air enthalpy at the entrance and exit of the ventilated façade.

$$U_{VF} = \sum(m_j \cdot c_{P_j} \cdot (T_j - T_0)) \tag{22}$$

$$\frac{dU_{VF}}{dt} \approx \frac{\Delta U_{VF}}{\Delta t} = \sum\left(m_j \cdot c_{P_j} \cdot \left(\frac{T_{j_t} - T_{j_{t-\Delta t}}}{\Delta t} - \frac{T_{0t} - T_{0t-\Delta t}}{\Delta t}\right)\right) \tag{23}$$

$$\dot{H}_{in} - \dot{H}_{out} = \dot{m}_{air}c_P(T_{in} - T_{out}) \tag{24}$$

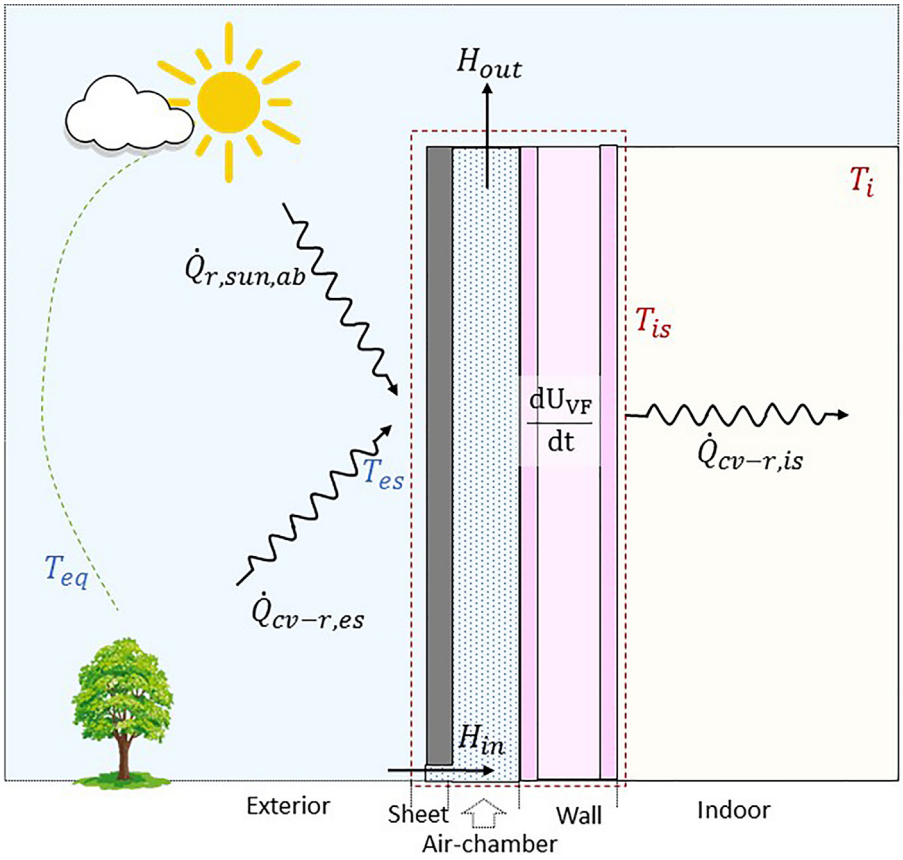

Fig. 3. Scheme of a simple ventilated façade (summer).

If an exergy balance is performed then:

$$\frac{dB_{VF}}{dt} = \dot{B}_{r,sun,ab} + \dot{Q}_{cv-r,es}\left(1-\frac{T_0}{T_{es}}\right) - \dot{Q}_{cv-r,is}\left(1-\frac{T_0}{T_{is}}\right) + \dot{B}_{in} - \dot{B}_{out} - \dot{D}_T \quad (25)$$

where $\dot{B}_{in} - \dot{B}_{out}$ is the exergy change of the air entering in the chamber ($\dot{B}_{in} - \dot{B}_{out} = \dot{m}_{air} \cdot c_{P_{air}} \cdot \left((T_{in} - T_{out}) - T_0 \ln\left(\frac{T_{in}}{T_{out}}\right)\right)$); $\dot{D}_T$ is the rate of total exergy destruction in the façade, including all the heat exchange mechanisms and the irreversibilities associated with the air flow in the chamber, and B_{VF} is the exergy accumulated in the materials:

$$B_{VF} = \sum \left[m_j \cdot ((u-u_0)j - T_0(s-s_0))j\right] = \sum \left[m_j \cdot c_{P_j} \cdot \left((T_j - T_0) - T_0 ln\left(\frac{T_j}{T_0}\right)\right)\right] \quad (26)$$

$$\frac{dB_{VF}}{dt} \approx \frac{\Delta B_{VF}}{\Delta t} = \sum \left[m_j \cdot c_{P_j} \cdot \left(\left(\frac{\Delta T_j}{\Delta t} - \frac{\Delta T_0}{\Delta t}\right) - \frac{\Delta T_0}{\Delta t}\ln\left(\frac{T_j}{T_0}\right) - T_0 \cdot \left(\frac{\frac{\Delta T_j}{\Delta t}T_0 - T_j\frac{\Delta T_0}{\Delta t}}{T_j \cdot T_0}\right)\right)\right] \quad (27)$$

4.2. Performance coefficients of a ventilated façade

As said in the literature review, no exergy index is found to characterize the thermal behavior of ventilated façades or roofs. The most common exergy indicators focus on industrial processes or energy generation systems. Among them, the following are found: the exergy efficiency used by Boelman & Sakupipatsin [33], and Cornelissen & Hirs [34], or the functional efficiency of Kotas [35] and Tsatsaronis [36].

Therefore, a coefficient to characterize the behavior of building envelopes needs to be defined in terms of exergy, particularly for VFs. Furthermore, this coefficient has to consider the envelope as a dynamic system and must be easy to interpret and not distant from the energy coefficients. Considering the requirements, the Doctoral Thesis of I. Flores [37] defines five possible parameters. After analyzing the results for different walls, climates, etc., the most interesting is the one based on the ISO 9869-1 standard expression [38], for the "in situ" determination of the thermal resistance of a wall, and is called "dynamic exergy transmittance".

In this work, a different point of view is adopted. In order to assess the interest of incorporating or not a VF, its thermal behavior is compared with that of a conventional façade that meets the minimum requirements required by the regulations, and therefore depending on the geographical area and climatic conditions.

Under the point of view of the first law, this work defines a coefficient that relates the energy lost through the conventional (reference) façade versus that lost in the VF. For winter conditions, which are the most relevant in our zone, the heat flow $\dot{Q}_{is} = A\,h_{cv-r,is}(T_i - T_{is})$ goes from the indoor air at T_i to the internal surface at T_{is}, being T_{is}^{ref} the internal surface temperature in the reference façade. The heat exchanged by the reference façade internal surface through convection and longwave radiation is $\dot{Q}_{is}^{ref} = A\,h_{cv-r,is}\left(T_i - T_{is}^{ref}\right)$, Fig. 4 (b).

This work proposes naming this ratio the *Energy Quality Coefficient (EQC)* so,

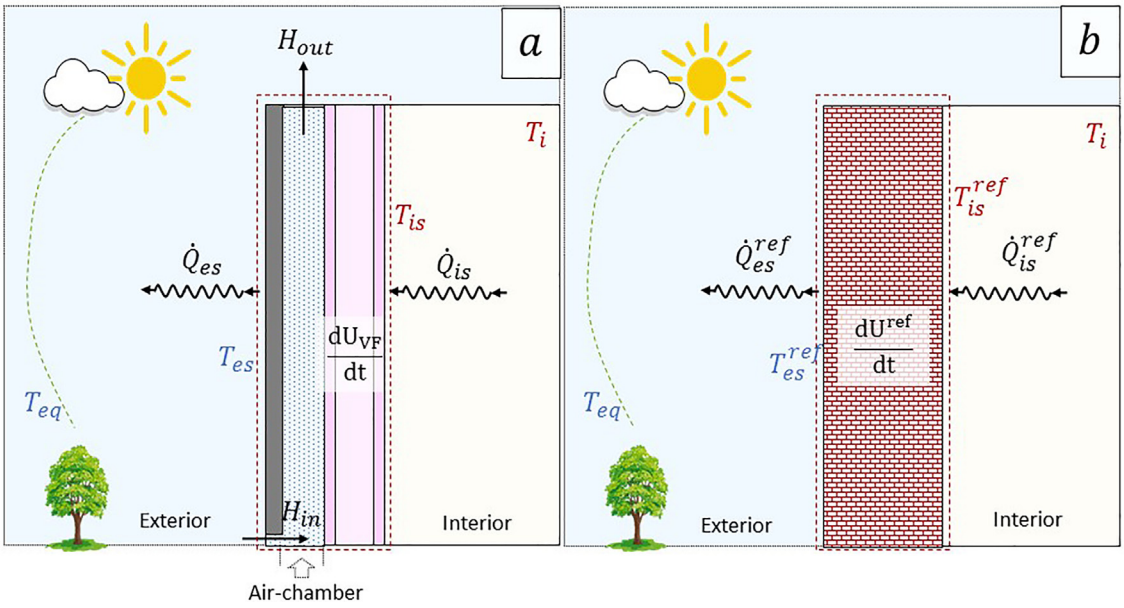

Fig. 4. (a) Energy loss in ventilated façade vs (b) reference façade.

$$EQC = \frac{\sum_{j=1}^{n} Q_{is_j}^{ref}}{\sum_{j=1}^{n} Q_{is_j}} \tag{28}$$

where $n = 1 \cdots j$ corresponds to the heat transferred during the n periods of time considered. Applying the energy balance, the above definition can be expressed with reference to the external surface "es", by considering in the term Q_{es_j} the solar absorption (Q_{r,sun,ab_j}) and the convection-radiation (Q_{cv-r,es_j}), then,

$$EQC = \frac{\sum_{j=1}^{n} \left[Q_{es_j}^{ref} + \Delta U_j^{ref} \right]}{\sum_{j=1}^{n} \left[Q_{es_j} + (H_{out} - H_{in})_j + \Delta U_j \right]} \tag{29}$$

If *EQC* is greater than one, the VF is thermally preferable to the reference-façade defined by the application of the Spanish Technical Code (CTE) limiting values. In winter conditions, if the pre-heated air of the chamber is used in the building, $H_{out} - H_{in}$ should appear in the denominator of eq. (28), so that $\sum_{j=1}^{n} Q_{is} - (H_{out} - H_{in})$ is now the heat-loss.

Comparing the exergy lost by such a reference-façade with the exergy lost by the VF, we can similarly define an *exergy quality coefficient ExQC*, as follows

$$ExQC = \frac{\sum_{j=1}^{n} Q_{is_j}^{ref} \left(1 - \frac{T_{0_j}}{T_{is_j}^{ref}} \right)}{\sum_{j=1}^{n} Q_{is_j} \left(1 - \frac{T_{0_j}}{T_{is_j}} \right)} \tag{30}$$

Referring this coefficient to the external surface "es" of the FV, through the exergy balance equation:

$$ExQC = \frac{\sum_{j=1}^{n} \left[B_{es_j}^{ref} + \Delta B_j^{ref} + D_j^{ref} \right]}{\sum_{j=1}^{n} \left[B_{es_j} + (B_{out} - B_{in})_j + \Delta B_{VF_j} + D_j \right]} \tag{31}$$

In summer, when $T_0 > T_{is}$, the heat flux-gain $\dot{Q}_{is}$ supposes an exergy output from indoor equal to $\dot{Q}_{is} \cdot \left(1 - \frac{T_0}{T_{is}}\right)$, so the heat flux and its corresponding exergy have opposite senses. The objective now is to reduce the heat flow $\dot{Q}_{is}$ so that the exergy associated with it and that goes out from the indoor air is as low as possible. In these conditions, the hot air in the chamber is sent outdoors.

5. Case study

5.1. Characteristics of the paslink cell-tests

PASLINK dynamic cell-tests are highly standardized tests that allow construction solutions to be thermally characterized under real dynamic conditions thanks to their numerous and strategic sensors. The development of PASLINK tests started more than 20 years ago, through international work coordinated and funded by EU research projects [39]. PASLINK cells consist of a test room where the sample to be tested is placed, and an adjacent service room where the heat exchange through the sample is measured with high precision, see Fig. 5.

5.2. Description of the forced ventilated façade tested

The construction-solution tested as the case study in the PASLINK cell is a light and industrialized ventilated façade with dry assembly and prefabricated materials, see Fig. 6. It is a simple façade consisting of a 2 mm galvanized steel sheet, a 3 cm air chamber and a sandwich panel with a 6 cm polyurethane core. The air inside the ventilated chamber moves in a forced way by means of three extraction hoppers located in the upper part of the sample.

Fig. 7 shows the location of the temperature sensors (Pt 100) in the various layers of the ventilated façade; as it can be seen, the air chamber has a calibrated thermopile with numerous sensors to measure the increase in the air temperature across it. In addition to the sensors in the sample there are: 12 Pt100 sensors for ambient temperature, 3 Kypp and Zonnen CMP11 Solarimeters to measure the total vertical and horizontal solar radiation and 1 shadow ring to measure diffuse radiation, 1 sensor for the outside wind direction and another one for its speed, 1 differential pressure meter, 1 air flow meter, and 1 power transducer.

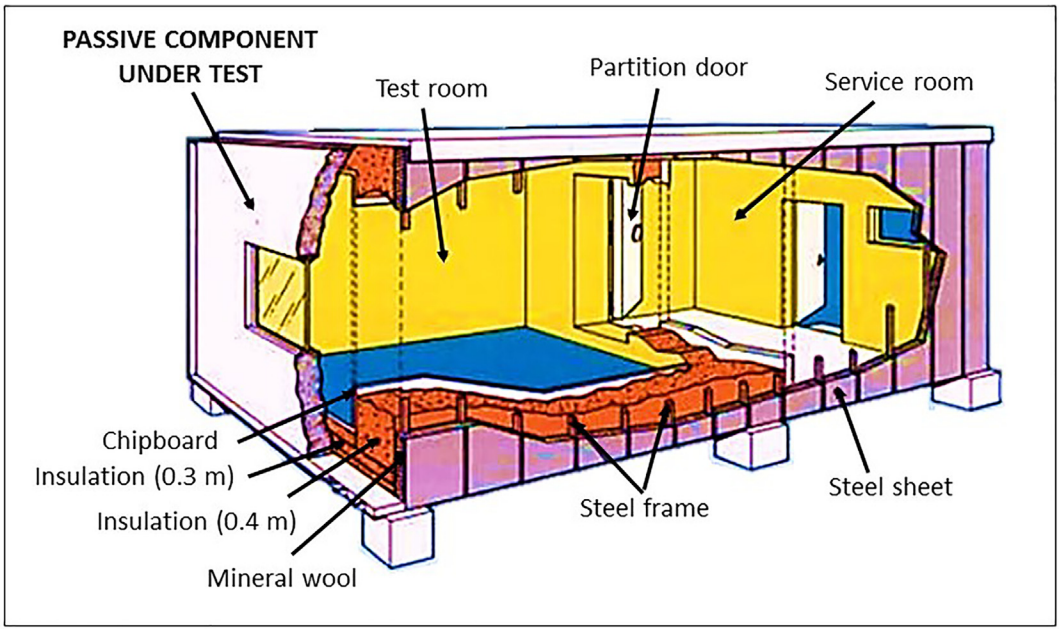

Fig. 5. Structure of a Paslink cell.

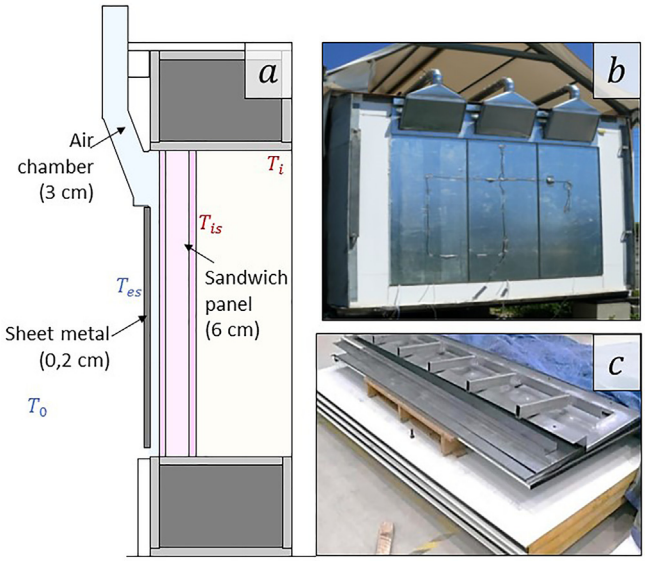

Fig. 6. (a) Layers of the ventilated façade, (b) PASLINK cell, (c) materials.

5.3. Data obtained from the test

The test was carried out at the Building Quality Control Laboratory of the Basque Government (LCCE) in Vitoria/Gasteiz, northern Spain, over 6 days (from November 8th to 13th) and data were collected every 10 min.

Fig. 8 shows the data collected directly from the sensors in each layer. All temperatures show a similar trend, which allows the values to be averaged to a single surface-temperature value (except for the air temperature inside the chamber, which increases its value vertically from T_{in} at the entrance to T_{out} at the exit).

The average standard deviations σ_{avg}, when averaging the temperatures for each surface at a single surface temperature $T_{s,j}$, are gathered in Table 2.

Fig. 9 shows the outdoor and indoor temperatures, and the average internal and external surface temperatures of the VF, as well as the solar irradiation (vertical global, horizontal global, and horizontal diffuse) and the airflow rate through the air chamber.

6. Results

This section shows the results of the analysis performed with the data obtained in the test. The results are presented in three sections: 6.1 Energy Analysis, 6.2 Exergy Analysis and 6.3 Performance Coefficients.

6.1. Energy analysis

This section contains the dynamic and global results of energy analysis.

6.1.1. Dynamic energy analysis of the VF

Calculating the components of the energy balance equation in the façade, eq. (20), the values obtained are shown in Fig. 10. The following trends are observed:

- When there is solar irradiation G_T, the external surface temperature T_{es} rises markedly, making $\dot{Q}_{cv-r,es}$ negative (i.e., loss) as $T_{eq} < T_{es}$;
- On the other hand, the air-flow temperature in the chamber rises from inlet T_{in} to outlet T_{out}, participating in the heat transfer, which makes $\dot{H}_{in} < \dot{H}_{out}$ and therefore preheating the air to be after inserted inside the house.
- Furthermore, as the coefficient $h_{cv-r,is}$ is low, there is hardly any temperature difference between the indoor temperature T_i and the internal surface temperature T_{is}. In addition, as $T_i > T_{is}$, $\dot{Q}_{cv-r,is}$flows outwards (it has a negative sign).
- When the solar radiation absorbed $\dot{Q}_{r,sun,ab}$rises and the external surface temperature T_{es} increases, the VF loses heat to the outside, so its internal energy decreases $\frac{dU_{VF}}{dt} < 0$. Fig. 11 justifies this fact by depicting the solar irradiation vs the change in inter-

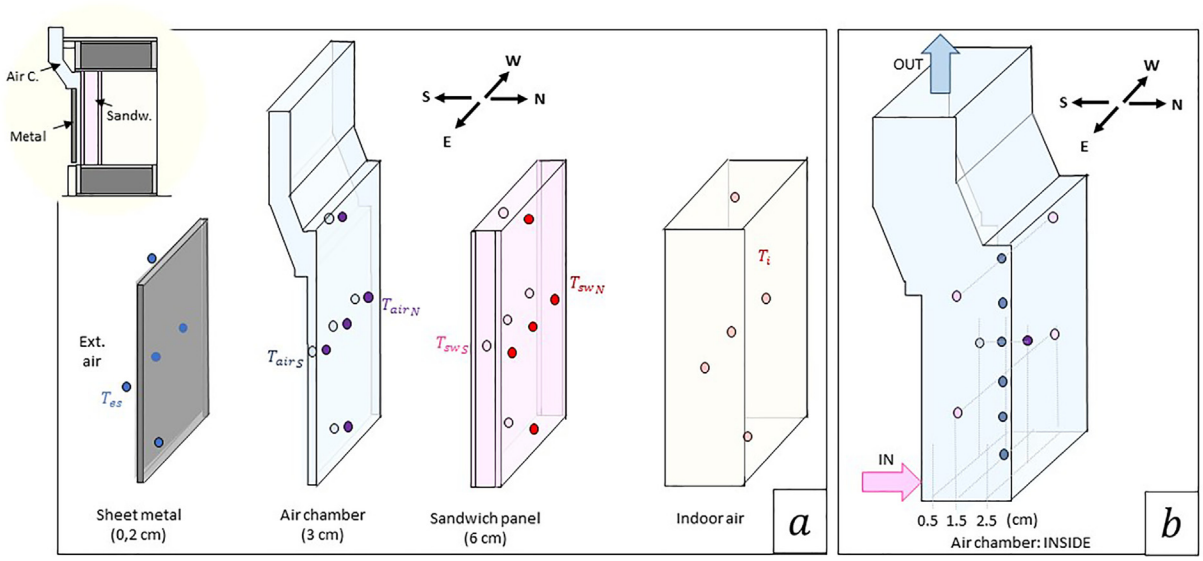

Fig. 7. a) Location of sensors in the different layers of the ventilated façade. b) Zoom in the inside of the air chamber.

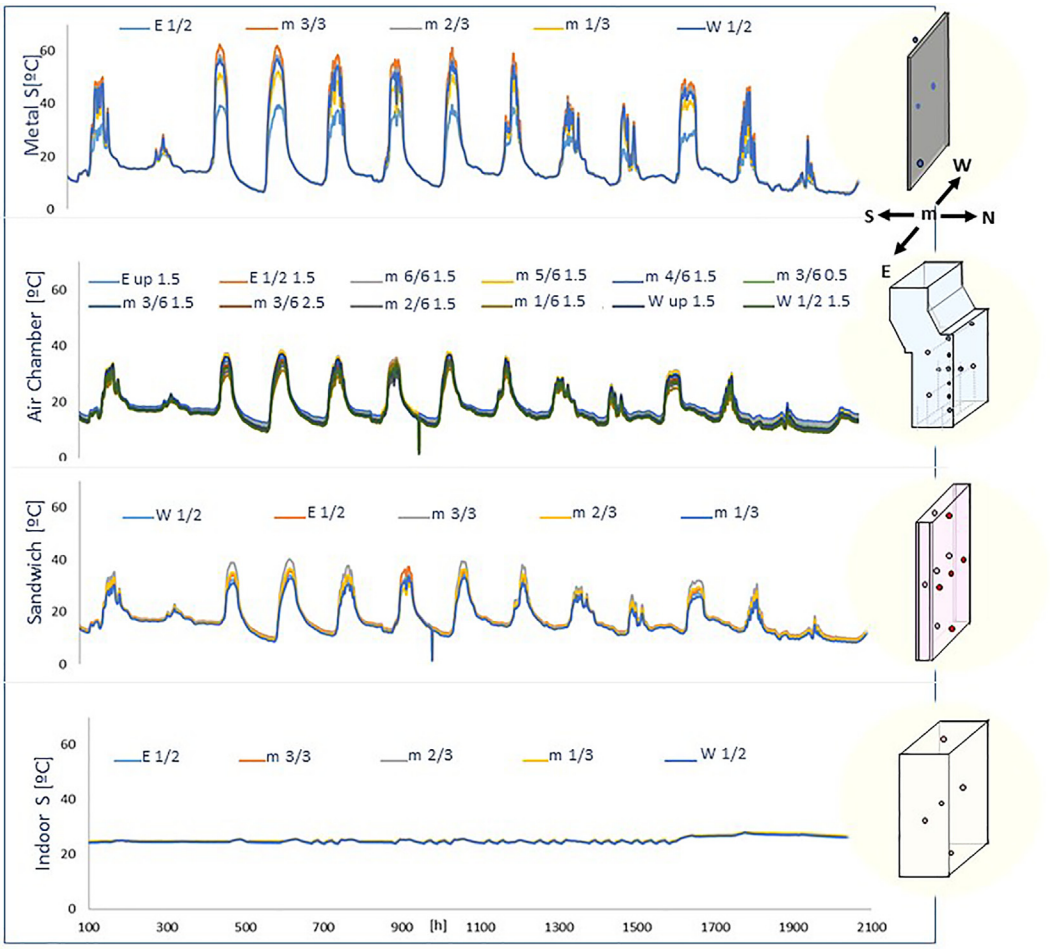

Fig. 8. Temperatures of each layer according to sensor location.

nal energy. It can be seen that the solar irradiation absorbed noticeably stimulates the internal energy increase and decrease of the VF.

6.1.2. Energy analysis of the VF over the test period

As a summary, Table 3 shows the accumulated energy during the 6-day test period for each of the energy balance terms.

Table 2
Average standard deviations in each surface.

	σ_{avg}[°C]
Metal S	0.828
Sandwich	1.098
Indoor S	0.176

As discussed in eq.(21), but in energy terms, the change of the internal energy in the VF is due to the energy balance between the flows coming from the exterior and the ones going indoor: $\Delta U_{VF} = Q_{r,sun,ab} + Q_{cv-r,es} - Q_{cv-r,is} - \Delta H_{air}$. Therefore, $Q_{r,sun,ab}$ and $Q_{cv-r,es}$ are considered to come from the exterior to the façade (increasing its internal energy) and $Q_{cv-r,is}$ and $\Delta H_{air} = H_{out} - H_{in}$ go from the façade to the interior of the building (decreasing U_{VF}).

- Thus, with the sign convention adopted, the overall $Q_{cv-r,es}$ during 6 days is negative, which means that it goes from the external surface to the exterior, i.e., is a loss.
- The contrary happens with $Q_{cv-r,is}$, which goes indeed from indoor to the internal surface.

In addition, Table 3 and Fig. 12 also gather the percentage of each energy-flow in as its contribution to the energy balance.

- The most important terms are $Q_{r,sun,ab}$ and $Q_{cv-r,es}$, which show that almost all the heat absorbed from the shortwave solar radiation in the façade surface is conversely counterbalanced by longwave convection-radiation that escapes to the exterior. These two effects together account for 87.85 % of the total heat transferred across the façade.
- The remaining 12.15 % is distributed among the $Q_{cv-r,is}$, ΔH_{air} and the decreasing ΔU_{VF}, being 87.36 % of this remaining energy the heated air flowing ΔH_{air} along the chamber.
- The internal energy of the façade hardly participates in the energy exchange (0.03 %) due to its low inertia and high thermal diffusivity of the metallic layer.

6.1.3. Dynamic energy analysis of the VF layers

Thanks to the PASLINK test-cell versatility, the work can be extended to the analysis of the façade layers energy behavior and the internal energy variation of the metal-sheet, the air chamber and the sandwich panel layers can be evaluated. Fig. 13 helps to visualize the dynamic behavior of each layer during the testing period. It is obvious to conclude that:

- The metal layer shows the biggest fluctuations in terms of internal energy change, since quickly loads and unloads because of its low thermal capacity. The sandwich panel follows it and, finally, the air chamber is the layer that dampens the heat-fluctuations the most due to its low density and dimensions.

6.1.4. Energy analysis of the VF layers over the test period

The previous dynamic analysis can be summarized by accumulating the internal energy variation of each layer over the 6-day testing-period, see Table 4 and Fig. 14. The following is observed:

- Almost all the internal energy variation (99.45 %) is due to the inertia of the sandwich panel. After all, it is the thickest ($t_{sandwich} = 6cm > t_{airC} = 3cm > t_{metalS} = 0.2cm$) and has the highest thermal capacity ($c_{Psandwich} = 1.8\frac{kJ}{kgK} > c_{PairC} = 1.005\frac{kJ}{kgK} > c_{PmetalS} = 0.39\frac{kJ}{kgK}$).
- The air chamber participates the less due to its low density ($\rho_{airC} = 1\frac{kg}{m^3} < \rho_{sandwich} = 100\frac{kg}{m^3} < c_{PmetalS} = 7850\frac{kg}{m^3}$).

6.2. Exergy analysis

In parallel with the above, this section presents the analysis results from the exergy point of view.

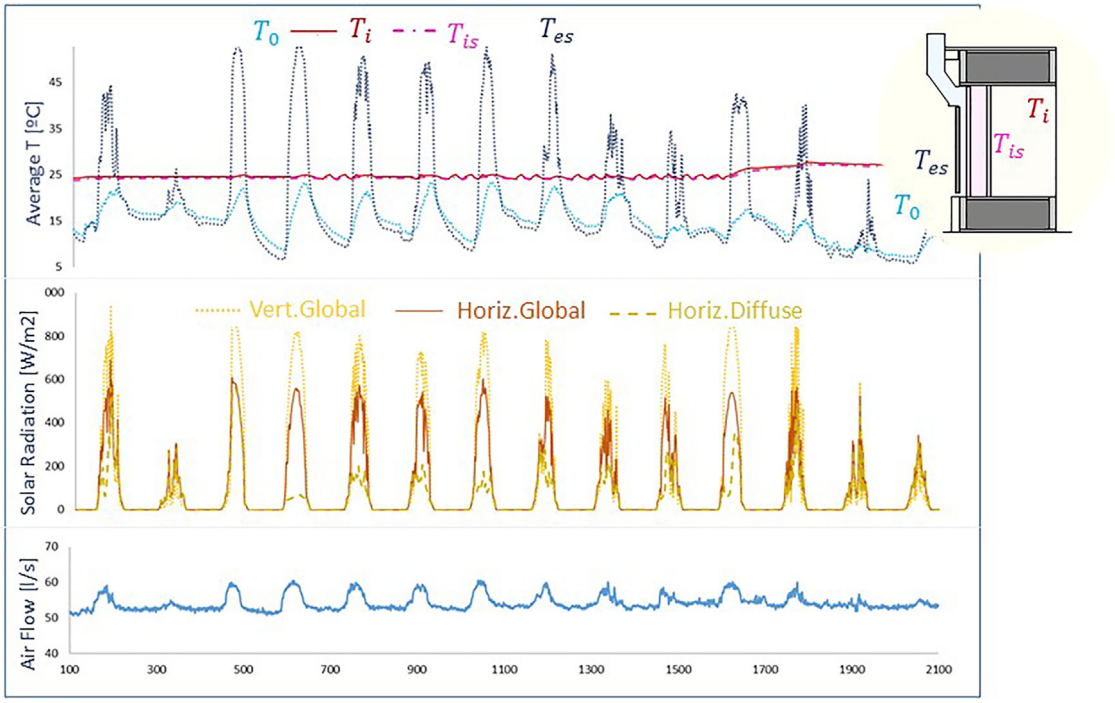

Fig. 9. Average surface temperatures, solar irradiation and airflow in the ventilated façade.

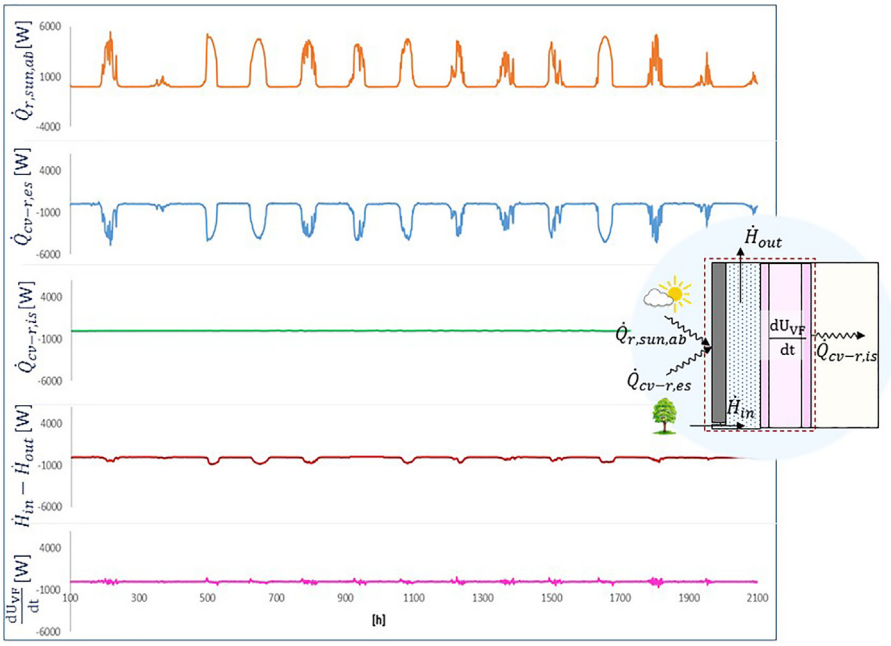

Fig. 10. Energy flows along the ventilated façade.

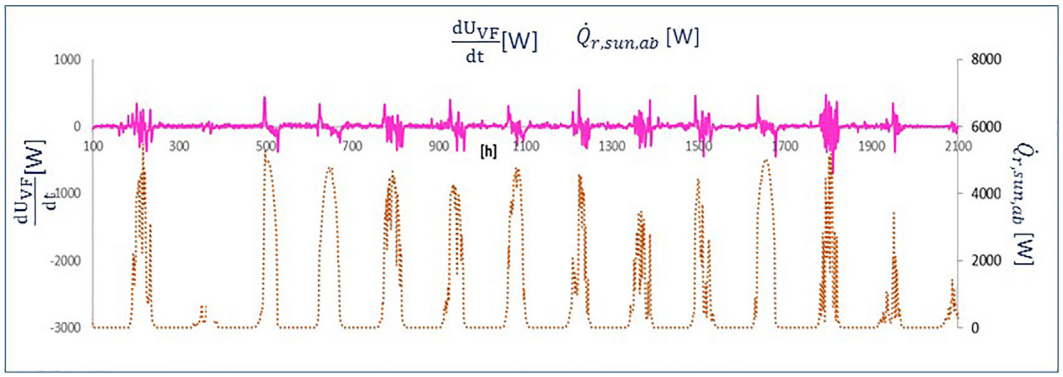

Fig. 11. Comparison between solar irradiation and internal energy variation.

Table 3
Energy in the test period and prcentage in the balance.

	Energy [kWh/6days]	[%]
$Q_{r,sun,ab}$	277.83	48.46
$Q_{cv-r,es}$	−225.78	39.39
$Q_{cv-r,is}$	−8.63	1.51
ΔH_{air}	60.85	10.61
ΔU_{VF}	−0.17	0.03

6.2.1. Dynamic exergy analysis of the VF

The results of the dynamic exergy analysis of the façade, following eq.(25), appear in Fig. 15. The trends are similar to those of the energy flows, although the scale of units decreases significantly. Likewise, the exergy destruction rate ($\dot{D}_T$) is also involved in this analysis.

- It should be noted that the y-axis scales of $\dot{D}_T$ and $\dot{B}_{r,sun,ab}$ are significantly larger than those of the other exergy fluxes. This is due to the fact that, following Petela [40], the exergy of solar absorbed radiation is obtained by multiplying the solar

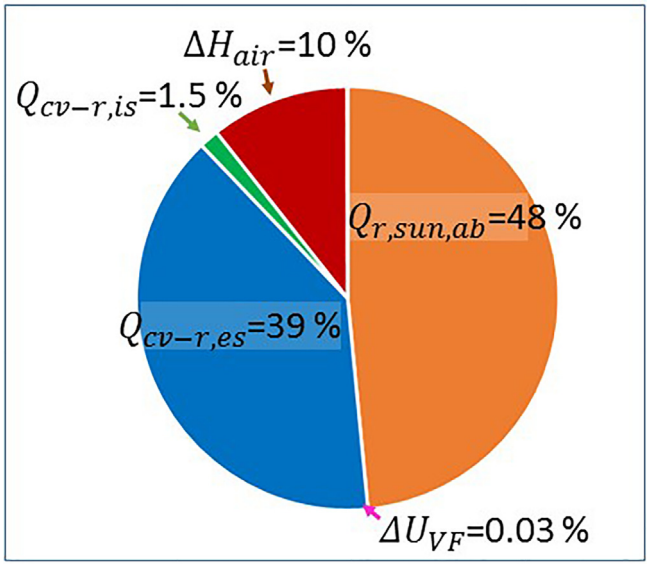

Fig. 12. Percentage of the energy balance.

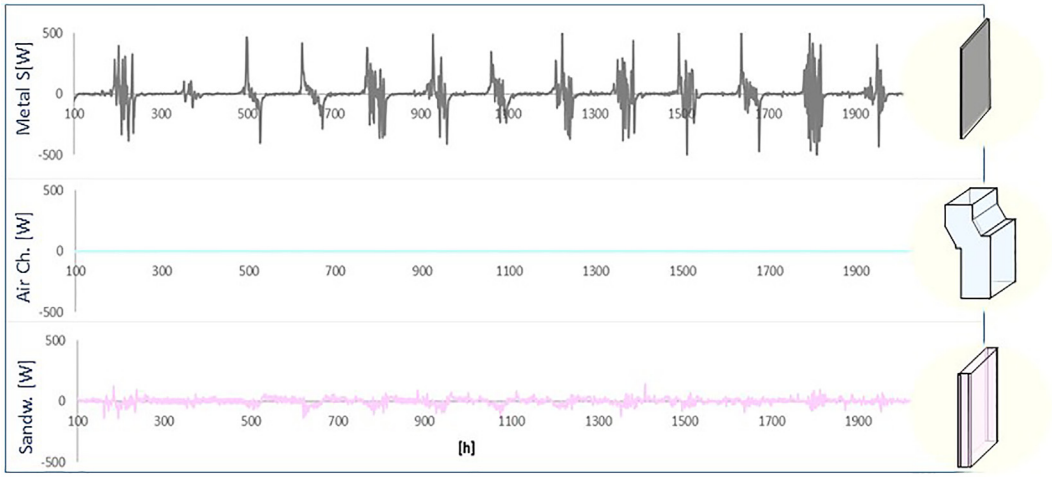

Fig. 13. Internal energy variation of the VF layers.

Table 4
Internal energy variation of the layers and percentage.

	$\Delta U_{VF,j}$[Wh/6days]	[%]
Metal sheet	−0.75	0.45
Air chamber	−0.15	0.09
Sandwich	−164.16	99.45

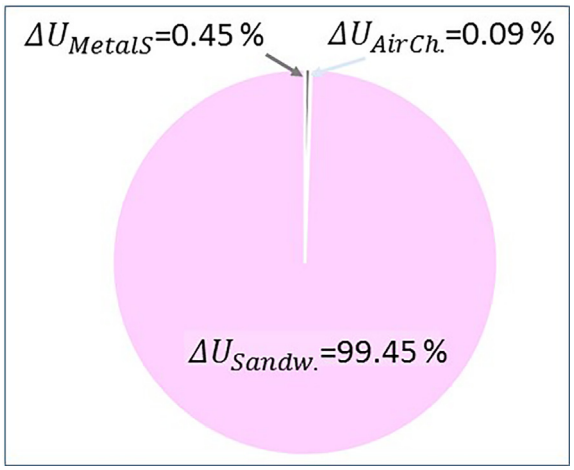

Fig. 14. Percentage E distribution of each layer.

absorbed radiation by its quality-factor $\left\{1+\frac{1}{3}\left(\frac{T_0}{T_{sun}}\right)^4-\frac{4}{3}\frac{T_0}{T_{sun}}\right\}$, which is close to unity. On the other hand, the temperatures at which heat exchanges take place by convection and longwave radiation and the thermomechanical exergy variation of the FV is close to the temperature T_0, and therefore they have a low exergy.

- For the same reason, almost all of the exergy from solar radiation is destroyed in the VF.

6.2.2. Exergy analysis of the VF over the test period

As a summary, Table 5 and Fig. 16 shows the accumulated exergy of each term of the exergy balance, eq.(25), over the 6-day test period.

- It is clearly shown that 94 % of the exergy of the solar absorbed radiation is destroyed and only 6 % of participates in the balance for exergy heat transfer.
- On the other hand, although from the energy point of view the terms $Q_{r,sun,ab}$ and $Q_{cv-r,es}$ are the most important, the same does not happen in terms of exergy. Now, the exergy of absorbed shortwave radiation from the sun $B_{r,sun,ab}$ is 17.4 times greater than the outgoing exergy from longwave convection-radiation $B_{cv-r,es}$. As mentioned above, this exergy is finally destroyed.
- Furthermore, even though the façade decreases the internal energy, the VF internal exergy variation is positive, moving away from the dead state condition.

6.2.3. Dynamic exergy analysis of the VF layers

The layer-by-layer dynamic exergy analysis shows the same trends as the energy analysis, but on a much smaller scale, given the reduced values of the thermomechanical exergy versus the internal energy.

6.2.4. Exergy analysis of the VF layers over the test period

Although exergy dynamic trends are similar to energy results, the same does not happen when the accumulated values over the test period are obtained, see Table 6 and Fig. 17.

- In the energy analysis the sandwich panel was practically the only one participating in the loading and unloading of the VF internal energy due to its thermal inertia. However, in terms of exergy, the metal sheet influences the most (83.66 %) followed by the sandwich panel (16.56 %).
- This happens because, given its high thermal conductivity, the temperatures reached by the metal are very high and are notably far from the reference state. Therefore, the energy loadings and unloadings which are energetically compensated, are not compensated exergetically, since the relationship with temperature is not linear but a logarithm appears.
- In any case, the ΔB_{VF} corresponds to the difference of the internal exergy between the end and the beginning of the testing period. Therefore, an increase of ΔB_{VF} means that the temperature of the façade have moved away from the reference conditions, either above or below the reference threshold.
- The air chamber does not either influence the VF inertia, either from an energy or an exergy point of view.

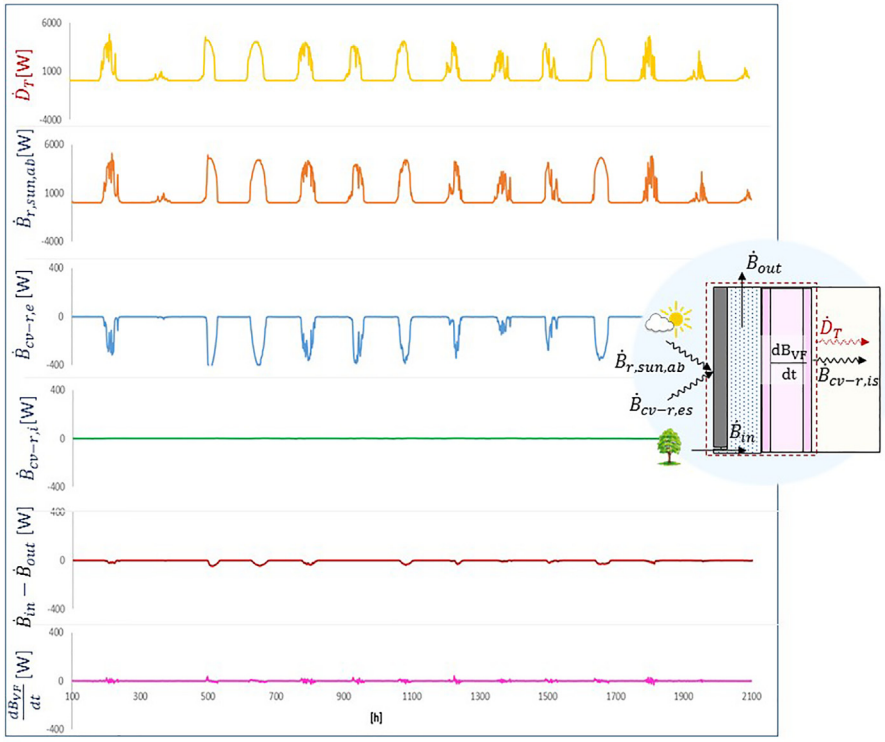

Fig. 15. Components of the VF exergy balance.

Table 5
Exaergy in the test period and percentage.

	Exergy [kWh/6days]	[%]
D_T	242.91	46.84
$B_{r,sun,ab}$	258.96	49.94
$B_{cv-r,es}$	−14.86	2.87
$B_{cv-r,is}$	−0.31	0.06
ΔB_{air}	1.40	0.27
ΔB_{VF}	0.10	0.02

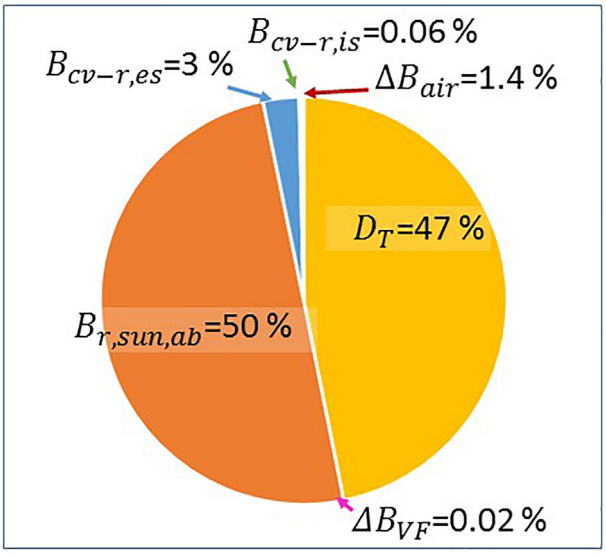

Fig. 16. Percentage of the exergy balance.

Table 6
Internal exergy varaition of the layers and percentages.

	$\Delta B_{VF,j}$[Wh/6days]	Percentage [%]
Metal sheet	85.31	83.66
Air chamber	0.10	0.10
Sandwich	16.56	16.24

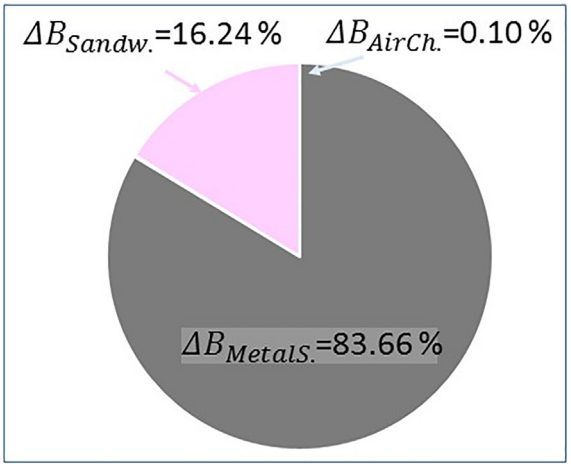

Fig. 17. Percentage B distribution of each layer.

6.3. Performance coefficients

As mentioned above, the benefit of a VF can be quantified by comparing it with a conventional reference-façade. As has been said, the reference-façade has been defined on the basis of the requirements of the Spanish Technical Building Code (CTE), which limits the maximum thermal transmittances for new buildings or

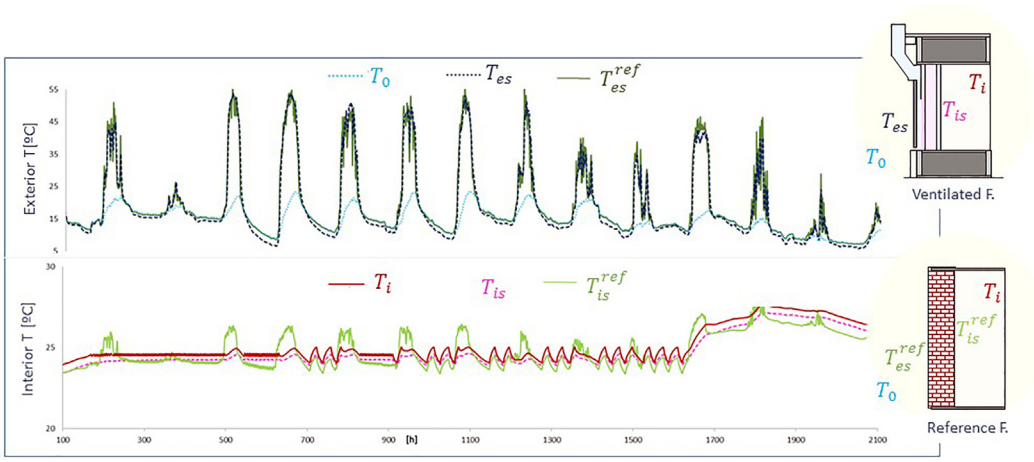

Fig. 18. Interior and exterior temperatures of ventilated façade and reference façade.

renovations, depending on the climatic zone. Thus, considering the composition of conventional façades within the "Catalogue of Building Elements" of the CTE [41], a façade with exposed masonry was chosen as a reference one, without an air chamber and with insulation on the inside. The global more restrictive thermal characteristics are as follows:

- Thermal maximum transmittance: $U_{lim} = 0.41 W/m^2K$
- Façade thickness (same as the VF): $L = L_{VF} = 0.092m$
- Specific heat of the reference-façade: $c_{P_{ref}} = 1000 J/kgK$
- Density of the reference-façade: $\rho_{ref} = 1150 \frac{kg}{m^3}$

Considering these characteristics and maintaining the same indoor T_i and outdoor T_0 temperatures, the surface temperatures T_{is}^{ref} and T_{es}^{ref} of the reference-façade are calculated. Fig. 18 depicts the VF surface temperatures vs the reference one.

- Surface exterior temperatures T_{es}^{ref} and T_{es} follow a very similar tendency.
- However, the ventilated air chamber in the VF makes the indoor T_{is} surface-temperature more stable, while T_{is}^{ref} fluctuates more. This behavior is due to the low thickness of the reference wall, with only 9.2 cm.

Considering the tested period from November 8th to 13th, the performance coefficients of eq.(28) and eq.(30) are calculated and shown in Table 7.

- As the EQC is slightly higher than one, the thermal behavior of the VF is slightly preferable to the reference-façade, but as the value is very close to one, one can interpret that both façades behave similarly.
- However, if the exergy point of view is adopted instead and the ExQC is calculated, the VF clearly has a better thermodynamic behavior than the reference one. The reason is that, as T_{is}^{ref} fluctuates more (especially when the sun irradiates and there is a heat flux to the interior), so T_{is}^{ref} goes further from T_0 and the factor $\left(1 - \frac{T_0}{T_{is}^{ref}}\right)$ is therefore greater than $\left(1 - \frac{T_0}{T_{is}}\right)$, meaning that a higher quality heat is lost through the reference wall, even if the EQC is close to 1.

Table 7
Energy and exergy performance coefficients.

EQC =	1.086
ExQC =	1.439

Therefore, the coefficient based on exergy, ExQC, takes into account the quality of the heat-flows, so it is a better index than EQC to identify the real losses across the walls.

7. Conclusions

This work analyses a VF from the perspective of the second law of thermodynamics through the exergy property. Exergy makes it possible to detect the real losses generated in any energy process, whether in active or passive systems.

The forced VF analyzed in this work is a prefabricated façade of light mass that has been tested experimentally during 6 days in the PASLINK cell of the Building Quality Control Laboratory, where more than 20 sensors collect data to characterize the layers of the façade. As the heat conduction is perpendicular to the wall, the layers can be considered at a homogeneous temperature at each time interval. It has been shown that the average standard deviation obtained by considering such a hypothesis is less than 1 °C. Nevertheless, the air chamber is characterized vertically and transversally, thanks to the 12 sensors along the chamber.

The dynamic energy analysis shows that, when there is solar irradiation, heat transfer occurs from the exterior surface to the interior. Nevertheless, in accumulated terms along the 6-day essay, almost all absorbed solar radiation is balanced ($Q_{r,sun,ab}$ = 277.83 kWh) by convection-radiation longwave losses ($Q_{cv-r,es}$ = 225.78 kWh) and also by the air enthalpy increment along the air chamber (ΔH_{air} = 60.85 kWh). Therefore, overall, 52.05 kWh of heat is lost to the outside through the façade during 6 days of November. The change of the internal energy in the VF (ΔU_{VF} = -0.17 kWh) is very small due to its low inertia, given its small thickness of 9.2 cm.

Thanks to the experimental test, each layer of the façade is analyzed individually and it is shown that the highest internal dynamic energy fluctuations occur in the metal-sheet, due to the low inertia and high thermal diffusivity of the material. Hence, almost all the internal energy variation (99.45 %) is due to the sandwich panel layer.

The exergy analysis shows the same trends, but on a much smaller scale, and includes the exergy-destruction term, which is

also one of the largest in the exergy balance. Thus, most of the exergy from solar radiation (94 %) is ultimately destroyed without being used inside the building. The exergy of exterior convection-radiation flow and the exergy-flows on the indoor side are almost negligible due to the closeness of their temperatures to the reference state (outdoor air). Therefore, although energetically the terms $Q_{r,sun,ab}$ and $Q_{cv-r,es}$ influence the most, the exergy absorbed from the sun $B_{r,sun,ab}$ is 17.4 times greater than $B_{cv-r,es}$.

Even if in energy terms the sandwich panel was the most influencing layer in ΔU_{VF}, in terms of exergy the metal sheet is the most important (83.66 %) followed by the sandwich panel (16.56 %) due to high temperature changes with respect to the reference state.

This information can only be obtained by applying the first and second laws of thermodynamics.

This work also proposes a new parameter to characterize the thermal behavior of façades, based on either energy EQC or exergy ExQC. Although the EQC index suggests that the VF and its unventilated reference-façade have a similar thermal performance (1.086), the ExQC shows that the exergy losses of the conventional façade are 44 % higher than those of the VF. Therefore, the index based on exergy provides information that would otherwise not be obtained with an energy-based.

8. Discussion

One of the limitations of this analysis is the lack of familiarity with the use of the exergy property in buildings applications. The results obtained are not as easy to interpret as those from energy analysis, where energy is conserved and only thermal losses participate in the efficiencies and neither "irreversibility" nor "destruction" terms appear. Furthermore, the exergy depends on the chosen reference state. The reference state in building analysis varies as environmental conditions change, which requires a dynamic approach (as it is also the case for energy analysis) and therefore a large amount of data is needed, which is often not easy or even impossible to obtain. Likewise, applying exergy analysis implies changing the point of view and penalizing energy transformations that convert high -quality into low- quality energy, as it is the case of solar radiation that converts into heat and therefore a large part of its exergy is destroyed. However, this work aims to go a step further in the work of encouraging the application of exergy analysis in buildings, focusing on forced ventilated façades, and justifying all the steps of its methodology and the results obtained.

As one of the main outcomes of this work, it can be concluded that the dynamic analysis of heat transfer through façades based on exergy requires the same data of those needed for energy analysis, since it is enough to know the temperatures at each surface and the thermal characteristics of each component. Therefore, if the required data are known, the energy analyses can be complemented with exergy analyses to obtain additional valuable information.

It has also been demonstrated that the importance of each heat flow varies greatly from one analysis to another, highlighting the need to link each flow to a common comparable baseline, which is the quality of the energy (i.e. exergy). In this way, the exergy balances point out the real exchanges involved in each transfer, demonstrating that the higher quality flows (solar gains) eventually end up being destroyed in the environment.

In addition, the implications that the energy and exergy variations of each façade layer are very different should be taken into account when designing the building envelope.

Last but not least, the ExQC coefficient is relatively simple to calculate and easy to interpret, so we suggest considering it for future analyses of façades and building envelopes in general.

Data availability

Data will be made available on request.

Declaration of Competing Interest

The authors declare that they have no known competing financial interests or personal relationships that could have appeared to influence the work reported in this paper.

Acknowledgments

The authors wish to express their gratitude for the support provided by the Building Quality Control Laboratory (LCCE) of the Basque Government, especially to JM. Hidalgo, C. Garcia-Gáfaro and D. Pérez for the help given throughout the test.

References

[1] D. D'Agostino, L. Mazzarella, What is a Nearly zero energy building? Overview, implementation and comparison of definitions, J. Build. Eng. 21 (2019) 200–212.
[2] M. Ibañez-Puy, M. Vidaurre-Arbizu, J.A. Sacristán-Fernández, C. Martín-Gómez, Opaque ventilated façades: thermal and energy performance review, Renew. Sustain. Energy Rev. 79 (2017) 180–191.
[3] T. Colinart, M. Bendouma, P. Glouannec, Building renovation with prefabricated ventilated façade element: a case study, Energ. Build. 186 (2019) 221–229.
[4] F. Ascione, N. Bianco, T. Iovane, M. Mastellone, G.M. Mauro, The evolution of building energy retrofit via double-skin and responsive façades: a review, Sol. Energy 224 (2021) 703–717.
[5] A. Gagliano, S. Aneli, Analysis of the energy performance of an Opaque Ventilated Façade under winter and summer weather conditions, Sol. Energy 205 (2020) 531–544.
[6] S. Shahrzad, B. Umberto, Parametric optimization of multifunctional integrated climate-responsive opaque and ventilated façades using CFD simulations, Appl. Therm. Eng. 204 (2022).
[7] A.C.F. Maciel, M.T. Carvalho, Methodology used to investigate the energy savings of opaque ventilated façades in residential buildings in Brazil, MethodsX 8 (2021).
[8] S. Fantucci, V. Serra, C. Carbonaro, An experimental sensitivity analysis on the summer thermal performance of an Opaque Ventilated Façade, Energ. Build. 225 (2020).
[9] F. Stazi, G. Ulpiani, M. Pergolini, C. Di Perna, M. D'Orazio, The role of wall layers properties on the thermal performance of ventilated façades: experimental investigation on narrow-cavity design, Energ. Build. 209 (2020).
[10] E. Pujadas-Gispert, M. Alsailani, K.C.A. van Dijk, A.D.K. Rozema, J.P. ten Hoope, C.C. Korevaar, S.P.G. Moonen, Design, construction, and thermal performance evaluation of an innovative bio-based ventilated façade, Front. Archit. Res. 9 (3) (2020) 681–696.
[11] R.F. De Masi, S. Ruggiero, G.P. Vanoli, Hygro-thermal performance of an opaque ventilated façade with recycled materials during wintertime, Energ. Build. 245 (2021).
[12] J.M. Sala-Lizarraga, A.P. Perez, Exergy Analysis and Thermoeconomics of Buildings: Design and Analysis for Sustainable Energy Systems, Butterworth-Heinemann, 2019.
[13] B.M. Ziapour, R. Dehnavi, Heat transfer in a large triangular-roof enclosure based on the second law analysis, Heat Mass Transf. 51 (7) (2015) 931–940.
[14] C. Biserni, M. Garai, First and second law analysis applied to building envelope: a theoretical approach on the potentiality of Bejan's theory, Energy Rep. 1 (2015) 181–183.
[15] V. Deshko, N. Buyak, I. Bilous, V. Voloshchuk, Reference state and exergy based dynamics analysis of energy performance of the "heat source-human-building envelope" system, Energy 200 (2020).
[16] F. Meggers, V. Ritter, P. Goffin, M. Baetschmann, H. Leibundgut, Low exergy building systems implementation, Energy 41 (1) (2012) 48–55.
[17] Y. Anand, S. Anand, A. Gupta, S. Tyagi, Building envelope performance with different insulating materials–An exergy approach, J. Therm. Eng. 1 (4) (2015) 433–439.
[18] A. Picallo-Perez, J.M. Hidalgo-Betanzos, J.M. Sala-Lizarraga. New Exergetic Methodology to Promote Improvements in nZEB. In Application of Exergy (p. 87). IntechOpen. 2018.
[19] A. Yildiz, A. Güngör, Energy and exergy analyses of space heating in buildings, Appl. Energy 86 (10) (2009) 1939–1948.
[20] A. Picallo-Perez, J.M. Sala-Lizarraga, E. Iribar-Solabarrieta, J.M. Hidalgo-Betanzos, A symbolic exergoeconomic study of a retrofitted heating and DHW facility, Sustainable Energy Technol. Assess. 27 (2018) 119–133.
[21] M.T. Balta, Y. Kalinci, A. Hepbasli, Evaluating a low exergy heating system from the power plant through the heat pump to the building envelope, Energ. Build. 40 (10) (2008) 1799–1804.

[22] S. Sayadi, G. Tsatsaronisb, T. Morosuk. (2016, June). A new approach for applying dynamic exergy analysis and exergoeconomics to a building envelope. In ECOS 2016: Proceedings of the 29th International Conference on Efficiency, Cost, Optimization, Simulation and environmental impact of energy systems (pp. 1-17).
[23] W. Choi, R. Ooka, M. Shukuya, Unsteady-state exergetic performance comparison of externally and internally insulated building envelopes, Int. J. Heat Mass Transf. 163 (2020).
[24] Y. Wang, A. Shukla, S. Liu, A state of art review on methodologies for heat transfer and energy flow characteristics of the active building envelopes, Renew. Sustain. Energy Rev. 78 (2017) 1102–1116.
[25] M. Debbarma, K. Sudhakar, P. Baredar, Thermal modeling, exergy analysis, performance of BIPV and BIPVT: a review, Renew. Sustain. Energy Rev. 73 (2017) 1276–1288.
[26] D. Kamthania, G.N. Tiwari, Energy and exergy analysis of semi transparent hybrid photovoltaic thermal double pass façade, Int. J. Renew. Energy Tech. 6 (2) (2015) 119–141.
[27] A.K. Shukla, K. Sudhakar, P. Baredar, Exergetic analysis of building integrated semitransparent photovoltaic module in clear sky condition at Bhopal India, Case Stud. Therm. Eng. 8 (2016) 142–151.
[28] A. Buonomano, F. Calise, A. Palombo, M. Vicidomini, Transient analysis, exergy and thermo-economic modelling of façade integrated photovoltaic/thermal solar collectors, Renew. Energy 137 (2019) 109–126.
[29] M. Borrallo-Jiménez, M. LopezDeAsiain, P.M. Esquivias, D. Delgado-Trujillo, Comparative study between the Passive House Standard in warm climates and Nearly Zero Energy Buildings under Spanish Technical Building Code in a dwelling design in Seville, Spain, Energy Build. 254 (2022).
[30] https://www.codigotecnico.org/pdf/Documentos/HE/DcmHE.pdf.
[31] D. Schmidt, H. Torio. ECBCS Annex 49. Low Exergy Systems for High-Performance Buildings and Communities, 182. 2011.
[32] H.A. Ahmed, T. Yu-xin, Y. Qi-chang, I.M. Al-Helal, M.R. Shady, A.M. Abdel-Ghany, Estimation of sky thermal irradiance in arid climate under clear sky conditions, Int. J. Thermophys. 41 (6) (2020) 1–18.
[33] E.C. Boelman, S. Popping. Critical analysis of exergy efficiency definitions applicable to buildings and building services. Tc, 10, 20. 2004.
[34] R.L. Cornelissen, G.G. Hirs, Exergetic optimisation of a heat exchanger, Energ. Conver. Manage. 38 (15–17) (1997) 1567–1576.
[35] T.J. Kotas, The Exergy Method of Thermal Plant Analysis, Paragon Publishing, 2012.
[36] G. Tsatsaronis, Definitions and nomenclature in exergy analysis and exergoeconomics, Energy 32 (4) (2007) 249–253.
[37] I. Flores Abascal. El método de análisis exergético en los edificios. Su aplicación en la caracterización en régimen dinámico de los cerramientos. 2016.
[38] D.S. Choi, M.J. Ko, Analysis of convergence characteristics of average method regulated by ISO 9869–1 for evaluating in situ thermal resistance and thermal transmittance of opaque exterior walls, Energies 12 (10) (2019) 1989.
[39] C. García-Gáfaro, C. Escudero-Revilla, I. Flores-Abascal, A. Erkoreka-González, K. Martín-Escudero, Dynamical edge effect factor determination for building components thermal characterization under outdoor test conditions in a PASLINK Test Cell: a methodological proposal, Energ. Build. 210 (2020).
[40] R. Petela, Exergy of undiluted thermal radiation, Sol. Energy 74 (6) (2003) 469–488.
[41] http://www.anape.es/pdf/Catalogo%20de%20Elementos%20Constructivos%20CAT-EC-v06.3_marzo_10.pdf.